Ultramicrotomy reveals the crystallographic information on the sectioned surface of the metallic block specimen

Adrian Mihai Sandu, Helmut Gnaegi, Johannes J.L. Mulders, Henny W. Zandbergen

Ultramicrotomy reveals the crystallographic information on the sectioned surface of the metallic block specimen

Journal:	*Philosophical Magazine & Philosophical Magazine Letters*
Manuscript ID:	TPHM-10-Feb-0055.R1
Journal Selection:	Philosophical Magazine
Date Submitted by the Author:	12-May-2010
Complete List of Authors:	SANDU, Adrian; Delft University of Technology, Faculty of Applied Sciences GNAEGI, Helmut; Diatome Ltd. MULDERS, Johannes; FEI Electron Optics ZANDBERGEN, Henny; Delft University of Technology, Faculty of Applied Sciences
Keywords:	dislocations, EBSD, TEM, SEM
Keywords (user supplied):	ultramicrotomy

Ultramicrotomy reveals the crystallographic information on the sectioned surface of the metallic block specimen

A.M. Sandu[1,2*], H. Gnaegi[3], J.J.L. Mulders[4] and H.W. Zandbergen[2]

1. Materials innovation institute (M2i), Mekelweg 2, Delft, NL-2628 CD, The Netherlands
2. Delft University of Technology, Faculty of Applied Sciences, Lorentzweg 1, Delft, NL-2628 CJ, The Netherlands
3. Diatome Ltd, Biel, CH-2501, Switzerland
4. FEI Electron Optics, Achtseweg Noord 5, NL-5600 KA Eindhoven, The Netherlands
** Corresponding author*

4 February 2010

Adrian M. SANDU
First name: Adrian
Middle name initial: M.
Family name: SANDU
Postal address work: Lorentzweg 1, NL-2628 CJ Delft, The Netherlands
Email address work: sandu@m2i.nl
Telephone number work: +31-15-278-4796
FAX number work: +31-15-278-6730

Helmut GNAEGI
First name: Helmut
Family name: GNAEGI
Postal address work: P.O. Box 1164, CH-2501 Biel, Switzerland
Email address work: helmut.gnaegi@diatome.ch
Telephone number work: +41-32-332-9113

Johannes J.L. MULDERS
First name: Johannes
Middle name initials: J.L.
Family name: MULDERS
Postal address work: Achtseweg Noord 5, NL-5600 MD Eindhoven, The Netherlands
Email address work: jjm@fei.com
Telephone number work: +31-40-235-6725

Henny W. ZANDBERGEN
First name: Henny
Middle name initial: W.
Family name: ZANDBERGEN
Postal address work: Lorentzweg 1, NL-2628 CJ Delft, The Netherlands
Email address work: h.w.zandbergen@tnw.tudelft.nl
Telephone number work: +31-15-278-2266

Abstract

Ultramicrotomy is widely regarded as a thin section preparation method for transmission electron microscopy (TEM) investigations. Here, we show that ultramicrotomy can also provide a simple path for microstructure analysis and assessment of mechanical properties for the sectioned face. Furthermore, electron backscatter diffraction (EBSD) analysis can be applied directly on ultramicrotomed surfaces without any additional polishing or etching. EBSD analysis relates the inherent cutting artifacts to the crystallographic orientations of the grains, hence delivering a rough assessment of their deformation resistance. TEM investigations revealed that crystallographic-related cutting artifacts, which exhibit a wave-like pattern, are the result of the dislocation pile-ups close to the knife-specimen interface. We consider that this technique is suitable to be coupled with EBSD for three-dimensional microstructure reconstructions when used for serial sectioning of large volumes.

Keywords

ultramicrotomy, electron backscattering diffraction, transmission electron microscopy, dislocations

1. Introduction

Microstructure is analyzed using classic techniques such as imaging a mechanically polished surface or a thin section in an optical (OM), scanning (SEM) and/or transmission electron microscope (TEM). However, many parameters of the complex microstructural features, such as connectivity, spatial distribution and true size and shape, cannot always be determined accurately from two-dimensional (2D) images [1] and require a three-dimensional (3D) approach.

Many of 3D visualization methods were initially developed by life sciences community, whereby they combined the *ex-situ* serial sectioning by ultramicrotomy with successive TEM imaging [2,3]. This laborious 3D technique was simplified when the serial ultramicrotomed block-face was directly imaged with an optical microscope. Surface imaging microscopy (SIM) [4] facilitated 3D sample reconstruction for larger volumes than those obtained by TEM. An increase in the resolution for both for biological and non-metallic materials, was achieved with the use of serial block-face scanning electron microscopy (SBFSEM) [5,6] which couples conventional SEM with *in-situ* ultramicrotome.

Comment [A1]: English check
Comment [A2]: English check
Comment [A3]: English check
Comment [A4]: English check
Comment [A5]: English check
Comment [A6]: English check
Comment [A7]: English check
Comment [A8]: English check

The primary tools for serial sectioning of metallic specimens are mechanical polishing [7,8] and recently, the focused ion beam (FIB) [9,10]. The latter was recently em ed and can be coupled with electron backscattering diffraction (EBSD) analysis which, however, requires a high-quality finish for the specimen surface since topographical features and/or preparation induced deformation may alter the Kikuchi pattern quality [11]. FIB sectioning delivers high surface finish for EBSD [9,10,12] but the procedure itself is time consuming when compared to the high data acquisition speed of the new [13-16] EBSD cameras.

Ultramicrotomy performs accurate serial sectioning over larger areas, while not subjecting the sectioned block-face to ion beam influences [17]. Here, we introduce ultramicrotomy sectioning as a fast sample preparation method that exposes the block-face microstructure of metallic specimens in just a few seconds and directly facilitates EBSD investigation. In particular what was investigated was whether the cutting artefacts hamper the EBSD analysis or lead to an undesired surface roughness. Also, we analyzed whether the cutting process pro microstructural surface features that can further speed up the 3D analysis process. For instance if grain boundaries can be displayed in SEM imaging then only a fraction of the sample surface needs to be analysed by EBSD because the shape of the grains can be determined from the grain boundary locations. We show, based on TEM and EBSD results, that most of the knife-induced strain is limited to the uppermost region of the block-face. Furthermore, we that grain boundaries are well displayed in SEM and optical microscopy and that some cutting effects can be used to quickly assess their deformation resistance in respect to the cutting direction. We theorize that all these can speed up the 3D grain analysis by a factor of 10^3, allowing for 3D analysis of large volumes (e.g. 200^3 μm^3) instead of the ~30^3 μm^3 that can be obtained using a FIB for sectioning.

Comment [A9]: English check

Comment [A10]: English check

Comment [A11]: English check

Comment [A12]: English check

Comment [A13]: English check

Comment [A14]: English check

Comment [A15]: English check

Comment [A16]: English check

2. Experimental procedure

A laboratory elaborated 6016 aluminium alloy containing 0.25-0.6 wt.% Mg, 1-1.5 wt.% Si was subjected to ultramicrotomy sectioning. The sample sectioning employed a Leica EM UC6 ultramicrotome using a Diatome ultra 35º diamond knife with a cutting speed of 30 mm/s. Rectangular specimens with the base parameter of 1 mm were polished to form a fine tip. 50 serial sections with 500 nm depth of cut were performed until a surface of the desired size was obtained at an undisturbed depth from the previous polishing. Afterwards, each specimen was sectioned with depths of cut of 30, 100, 500, 1000 and 5000 nm, respectively. The average roughness (R_a) of the ultramicrotomed block-faces was measured with a Veeco WYKO 3300 interferometer. The SEM investigations were performed using a FEI Strata 235 DB operated at 10 kV. The EBSD analysis was carried out at an accelerating voltage of 25 kV with a scan step size of 250 nm on a sample tilted 70º. Electron transparent lamellas for TEM observations were prepared via the focused ion beam method and investigated with a Philips CM30T microscope operated at 300 kV.

Comment [A17]: English check

Comment [A18]: English check

3. Results and discussion

3.1 Scanning electron microscopy / electron backscattered diffraction investigations

Figure 1(a) shows a SEM micrograph for the block-face specimen after ultramicrotomy sectioning at a feed (depth of cut) of 30 nm. The EBSD scanned area (40 x 10 μm^2) is marked with a white rectangle which includes a knife-induced groove and a few fine scratches (the white arrows). Figure 1(b) exhibits the EBSD orientation map from three grains marked as "A", "B", "C" revealing the existence of sharp grain boundaries. The groove position is indicated by the high number of randomly indexed points. Figure 1(c) shows the image quality (IQ) map which describes the sharpness of the Kikuchi bands. The patterns may become diffuse due to distortions of the crystal lattice induced by dislocations or precipitates

Comment [A19]: Additional change

Comment [A20]: English check

[18]. In the experiment the analyzed grains exhibit light grey to white IQ values indicating high quality of the Kikuchi patterns, with the grain boundaries showing up as dark grey to black since they exhibit lower IQs. This is related to the diffraction volume at the grain boundary which contains the crystal lattices of the neighbouring grains and hence a mix of the two patterns.

Figure 2(a) shows the SEM micrograph for the block-face specimen after ultramicrotomy sectioning at a feed of 1 μm. The EBSD scanned area (48 x 18 μm^2) is marked with a white rectangle and includes a wave-like feature as indicated by the white arrow. In the orientation map (Fig. 2(b)), five grains were identified: “D”, “E” - area marked by white arrow in Fig. 2(a), “F”, “G” and “H” respectively. The IQ map (Fig. 2(c)) also exhibits easily identifiable grain boundaries since, as mentioned before, they have lower IQs than the grains. The IQs for grains “E” and “F” exhibit a cyclic variation from lighter to darker grey with a wavelength of 1 μm. These “waves” are oriented perpendicular to the cutting direction and their arrangement resembles the wave-like feature indicated in Fig. 2(a). They may be associated to the local internal strains found within 40 nm below the sample surface which constitutes the diffraction volume [19]. The diffraction volume is a function of the electron beam diameter, the applied accelerating voltage, the specimen atomic number and its tilt angle during EBSD analysis. Typically, the specimen surface makes a 20° angle in respect to the incident beam. For this high tilt, the depth reached by the electron probe is between 10 to 40 nm [19]. Therefore, the backscattered electrons that generate the Kikuchi patterns, escape the specimen surface relatively undeviated after few inelastic scattering events [19]. In the case of grain “H”, the relatively high IQ values suggest a rather limited knife-induced strain at the cutting interface and hence also in the sampled diffraction volume.

Comment [A21]: English check

Comment [A22]: English check

Comment [A23]: English check

Comment [A24]: Additional change

Comment [A25]: English check

Comment [A26]: Referee comment number 2

Comment [A27]: Referee comment number 2

Comment [A28]: Referee comment number 2

3.2 Light interference microscopy investigations

The topography of the block-face specimen after ultramicrotomy sectioning at a feed of 30 nm is investigated in Fig. 3(a) by light interference analysis. The average roughness (R_a) is 11 ±13 nm which is comparable to lapping [20] ~10 nm, electrolytic abrasion (~25 nm) or super finishing [21]. Some grains ("B" and "C") exhibit different heights with respect to each other, therefore a surface profile measurement was performed (black line in Fig. 3(a)). In Fig 3(b), the left side of the plot represents the surface profile of grain "B" which exhibits most of its values above the reference line ($P_h = 0$). The right side of the plot originates from grain "C" and most of its values are under the reference line. The average difference in height between these grains is 13 nm. A bulge-dimple feature is marked at the grain boundary by the black triangle in Fig. 3(b). The height difference between the top of the bulge (grain "B" side) and the bottom of the dimple (grain "C" side) is 30 nm. The width of the dimple is ~2 µm.

The topography of the block-face specimen after ultramicrotomy sectioning at a feed of 1 µm is exhibited in Fig. 3(c). The R_a is 8 ± 14 nm and is comparable with the one obtained after sectioning at a feed of 30 nm. The grains boundaries can be identified along with some wave-like features marked with white arrows. Figure 3(d) presents the line profile of a wave-like feature (indicated by the black line in Fig. 3(c)) while the positions of the grain boundaries are indicated by black triangles. Between the grain boundaries there appears a pronounced rippling of the grain surface which corresponds to the wave-like pattern. The wave has a wavelength of ~1 µm and the peak-valley difference varies from ~ 5 nm to ~ 20 nm. Similar fluctuations [22] were reported in thin TEM sections of aluminium prepared by ultramicrotomy. A periodic change of the section's thickness with a wavelength of approximately 1 µm was observed.

Comment [A29]: Additional change

Comment [A30]: English check

Comment [A31]: Additional change

Comment [A32]: Additional change

Comment [A33]: English check

Comment [A34]: English check

3.3 Analysis of the knife-induced cutting artefacts

Studies on the microcutting of aluminium single crystals [23-26] have shown that a change in cutting direction with respect to crystal orientation leads to a change in the values of the cutting forces that dictate the surface finish. For instance, the cutting force was lower when cutting was performed parallel to {001} planes along [010] direction, compared to cutting along the [110] direction [22]. One may interpret these results as a change in the deformation resistance of the single crystal with respect to the cutting direction. Hence, given that our specimens are polycrystalline materials, one may expect each grain to have different cutting behaviour. We can analyze this process through a simple shear deformation, whereby each grain is considered as a single crystal with respect to cutting direction. The orientation of a given crystal, in regards to the cutting direction, can be described by an orientation factor [27] **m** whose higher absolute values show for what specific slip system the grain deforms easier:

$$m = \cos k * \cos\Theta * \cos\alpha + \sin k * \cos 2\Theta * \sin\alpha \quad (1)$$

where: k is the angle between the slip direction of the considered crystallographic system in the grain and the direction of the applied stress, Θ is the angle between the normal to the shear plane and the axis perpendicular to the sample surface (or grain surface in this case) and α is the angle between the applied stress direction and one of the axes of the sample coordinate system. Now, considering that α is zero *i.e.* the applied stress direction is parallel to sample surface, the formula becomes:

$$m = -\cos k * \cos\Theta \quad (2)$$

The analysis of the **m** values (see Supplementary information – Table 1) after sectioning at a feed of 30 nm revealed that grain "C" deformed the easiest, followed by grain "A" and grain "B". This analysis shows that the larger height of the grain "B" is related to an

Comment [A35]: English check

Comment [A36]: English check

Comment [A37]: Additional change

Comment [A38]: English check

elastic recovery following the knife passing its position, as seen in other investigations regarding nanometric cutting [28]. Moreover, the dimple is on the "softer" grain "C" side, while the bulge is on the "harder" grain "B" side (Fig 3(a)). This effect is observed in steels, at the interface between the harder pearlite and the softer ferrite [29]. The analysis of **m** after sectioning at a feed of 1 μm indicated that grain "E" opposed more to the deformation than grain "F". Therefore, the wave-like features occurred predominantly in the grains with a higher deformation resistance (white arrows in Fig. 3(c)).

Comment [A39]: English check

Comment [A40]: Additional change

Comment [A41]: Correction of the text explanation and its corresponding figure. Changed from Fig. 3(b) to Fig. 3(c).

3.4 Transmission electron microscopy observations on cross sections of microtomed surfaces

Figure 4(a) exhibits a bright field TEM micrograph of the top region of the sample after ultramicrotomy sectioning at a feed of 500 nm revealing a relatively low dislocation density in its bulk. Some dislocations that exceed 1.5 μm in length (white single-headed arrows) originate close to the knife-specimen interface and are oriented parallel to $<2\ -2\ 0>_{Al}$ directions. Figure 4(b) presents the knife-specimen interface of an area containing some wave-like features. This interface exhibits a high density of dislocation pile-ups aligned parallel to the cutting direction. They are discontinuous along the cutting interface at depths ranging between 75 to 150 nm. Other pile-up dislocations run parallel to the cutting interface at depths between 200 and 300 nm (double-headed arrows in Fig. 4(a-d)) on the entire length of the TEM specimen.

Comment [A42]: Additional change

Comment [A43]: English check

Figure 4(d) exhibits a relatively "flat" top-region of the specimen with a lower density of dislocations close to the cutting interface when compared to the wave-like feature region. Dislocation pile-ups aligned parallel to the top surface are found at a depth of ~ 200 nm with no dislocations running along $<2\ -2\ 0>_{Al}$ directions are present. Thus, it may be inferred that the line dislocations are associated to the presence of the wave-like features presence. The overall assessment of the knife-induced strain in the sample's bulk is given by the selected

Comment [A44]: English check

Comment [A45]: English check

area diffraction pattern (the inset in Fig. 4(d)) which exhibits sharp and undistorted reflections. This is an indication that the high dislocation density at the cutting interface does not change significantly the overall lattice orientation of the bulk grain which is sampled by the electron probe during EBSD analysis.

TEM observations revealed that for a "smooth" area, the knife-induced strain (such as dislocation pile-ups) is located beneath the depth of the diffracting volume for EBSD and does not affect the quality of the Kikuchi patterns. Therefore, the EBSD image quality map does not exhibit any variation of the grey levels, as it was also seen after 30 nm sectioning in Fig. 1. In the case of the "wave-like feature" the dislocations pile-ups accommodate part of the induced strain close to the cutting interface. They do not form a continuous damaged region and their depth also varies, in some cases being within the diffracting volume for EBSD. Thus, the strain sensitive IQ map exhibits periodic features, as shown in Fig. 2(c) for the grains "E", "F" and "G".

Comment [A46]: Referee comment number 1

Comment [A47]: Referee comment number 2 initial location. The answer is given in page 5.

4. Conclusions

We have shown that EBSD maps can be obtained directly from the aluminium block-face specimens sectioned on an ultramicrotome for depths of cut up to 1 μm and were not hampered by inherent cutting artefacts. They are related to the relative orientation of the grains with respect to the cutting direction. The grain boundaries are clearly visible and this facilitates a precise control of depth of the subsequent serial sectioning when removing grain/grains with certain orientations, in the particular case of aluminium alloys. TEM observations showed the "smooth" surfaces exhibit pile-up dislocations at a depth of 200 - 300 nm whereas the wave-like features consist of pile-up dislocations within 150 nm from the cutting interface, influencing the IQ maps. The mechanical properties of the grains can be readily assessed for low depth of cut based on the slight difference with respect to each other.

Comment [A48]: Referee comment number 3

Comment [A49]: Additional change

Comment [A50]: Referee comment number 3

Comment [A51]: English check

For higher depth of cut the mechanical properties of the grains can be assessed based on the wave-like patterns. Ultramicrotomy sectioning is a technique with high potential for microstructure analysis of the metallic materials, in particular for aluminium specimens which require relatively large volumes to be serial sectioned in a short time. The enhanced grain boundary visibility makes easier the control of serial sectioning in order to expose a certain grain. This technique can be potentially devised in a computer-controlled automated set-up which contains an in-situ ultramicrotome, a SEM and/or EBSD for imaging and a FIB for eventual removal of the strained region of the block-face after cutting, since other metallic materials may exhibit different deformation behaviours.

Comment [A52]: English check

Comment [A53]: Referee comment number 3

Comment [A54]: English check

Comment [A55]: Referee comment number 3

Acknowledgments
This research was carried out under the project number MC7.05209 in the framework of the Research Program of the Materials innovation institute M2i (www.m2i.nl). The authors would like to thank Prof. Leo Kestens and Dr. Jurij Sidor (TU Delft) for supplying the study material. A.M.S acknowledges the helpful discussions with Dr. Octav Paul Ciuca of the Toyohashi University of Technology / National Institute for Materials Science, Japan.

Comment [A56]: English check

References

[1] R.T. DeHoff, J. of Microsc. 131 (1983) 259.
[2] J.K. Stevens, T.L. Davis, N. Friedman, P. Sterling, Brain Res. Rev. 2 (1980) 265.
[3] K.M. Harris, Curr. Opin. Neurobiol. 9 (1999) 343.
[4] A. J. Ewald, H. Mcbride, M. Reddington, S. E. Fraser, R. Kerschmann, Developm. Dyn. 225 (2002) 369.
[5] W. Denk, H. Horstmann, PLoS Biol 2 (11) (2004) 1900.
[6] A. Zankel, B. Kraus, P. Poelt, M. Schaffer, E. Ingolic, J.of Microsc. 233 (2009) 140.
[7] T. Yokomizo, M. Enomoto, O. Umezawa, G. Spanos, R.O. Rosenberg, Mater. Sci. Eng. A 344 (2003) 261.
[8] A.C Lewis, J.F. Bingert, D.J. Rowenhorst, A. Gupta, A.B. Geltmacher, G. Spanos, Mater. Sci. Eng. A 418 (2006) 11.
[9] W. Xu, M. Ferry, J.M. Cairney, F.J. Humphreys, Acta Mater. 55 (2007) 5157.
[10] M.D. Uchic, L. Holzer, B.J. Inkson, E. L. Principe, P. Munroe, MRS Bulletin 32 (2007) 408.
[11] M. M. Nowell, R. A. Witt, B. True, Microsc. Microanal. 11(2) (2005) 504.
[12] N. Mateescu, M. Ferry, W. Xu, J.M. Cairney, Mater. Chem. and Phys. 106 (2007) 142.
[13] http://www.edax.com/snippet.cfm?Snippet_Id=1536
[14] http://www.oxinst.com/products/microanalysis/ebsd/detectors/Pages/nordlys.aspx
[15] http://www.bruker-axs.de/crystalign-ebsd.html
[16] http://www.nordif.com/?cat=2

[17] C. Quintana, Micron 28 (1997) 217.
[18] S.T. Wardle, L.S. Lin, A. Cetel, B.L. Adams, Proc. of 52nd Annual Meeting of the Microsc. Soc. of America (1994) 680.
[19] Randle, Adv. in Imag. and Electr. Phys. 151 (2008) 363.
[20] M.F. Ashby, Materials Selection in Mechanical Design: Third Edition. Butterworth-Heinemann Publish. House (2005) 200.
[21] Japanese industrial standard JIS B 0031 Geometrical Product Specifications (GPS) - Indication of surface texture in technical product documentation (1994).
[22] M. Ahlers, L.F. Vassamillet, J. of Appl. Phys. 39 (1968) 3592.
[23] M. Sato, T. Yamazaki, M. Kubo, Trans. of JIM 26 (1985) 251.
[24] M. Sato, T. Yamazaki, Y. Shimizu, T. Takabayashi, JSME Internat. J. 34 (1991) 540.
[25] S. To, W.B. Lee, C.Y. Chan, J. of Mater. Process. Tech. 63 (1997) 157.
[26] Z.J. Yuan, W.B. Lee, Y.X. Yao, M. Zhou, Annals of CIRP, 43 (1994) 39.
[27] J.P. Hirth, J. Lothe, Theory of Dislocations - 2nd edition. Wiley Publ. House, New York, (1982) 287.
[28] R. Komanduri, N. Chandrasekaran, L.M. Raff, Wear 242 (2000) 60.
[29] A. Simoneau, E. Ng, M.A. Elbestawi, Int.. J. of Mach. Tools and Manufact. 46 (2006) 1378.

Figure captions

Figure 1 SEM/EBSD investigations for the block-face specimen after ultramicrotomy sectioning at a feed of 30 nm: (a) SEM micrograph tilted 70º indicating the scanned area by EBSD (white rectangle) and marking some knife induced scratches (white arrows); the difference in image contrast is given by electron beam contamination of the sample surface such as the circular features; (b) tilt corrected orientation map [001]; (c) tilt corrected IQ map. The black line indicates the cutting direction.

Figure 2 SEM/EBSD investigations for the block-face specimen after ultramicrotomy sectioning at a feed of 1 µm: (a) Series of three consecutive (the white triangles mark the stitching lines) SEM micrographs tilted 70º indicating the scanned area by EBSD (white rectangle); some regions with different contrasts are given by electron beam contamination of the sample surface; (b) tilt corrected orientation map [001]; (c) tilt corrected IQ map. The black line indicates the cutting direction.

Figure 3 Light interference micrograph and the line profile analysis for the block-face specimens after ultramicrotomy cutting: (a) 3D reconstruction of the sample surface after ultramicrotomy sectioning at a feed of 30 nm; (b) line profile of an area crossing a grain boundary (black bar in (a)); (c) 3D reconstruction of the sample surface after specimen after ultramicrotomy sectioning at a feed of 1 µm; (d) line profile of an area containing a wave-like feature (black bar in (c)). The black lines indicate the cutting direction.

Figure 4 TEM investigations for the block-face specimen after ultramicrotomy sectioning at a feed of 500 nm: (a) bright field micrograph of the cross-sectioned area; (b) high magnification TEM micrograph of a “wave-like feature”; (c) simplified sketch of dislocations distribution in (b) where light grey is Pt layer, black is 6016 Al alloy and white are the dislocations; (d) high magnification TEM micrograph of a “flat” area and selected area diffraction pattern as inset (e^- // $[\bar{1}01]_{Al}$) of the areas in (a), (b) and (d).

Comment [A57]: Referee comment number 2
Comment [A58]: Additional change
Comment [A59]: Referee comment number 4
Comment [A60]: Additional change
Comment [A61]: Referee comment number 4
Comment [A62]: Additional change
Comment [A63]: Additional change
Comment [A64]: Referee comment number 4
Comment [A65]: Additional change

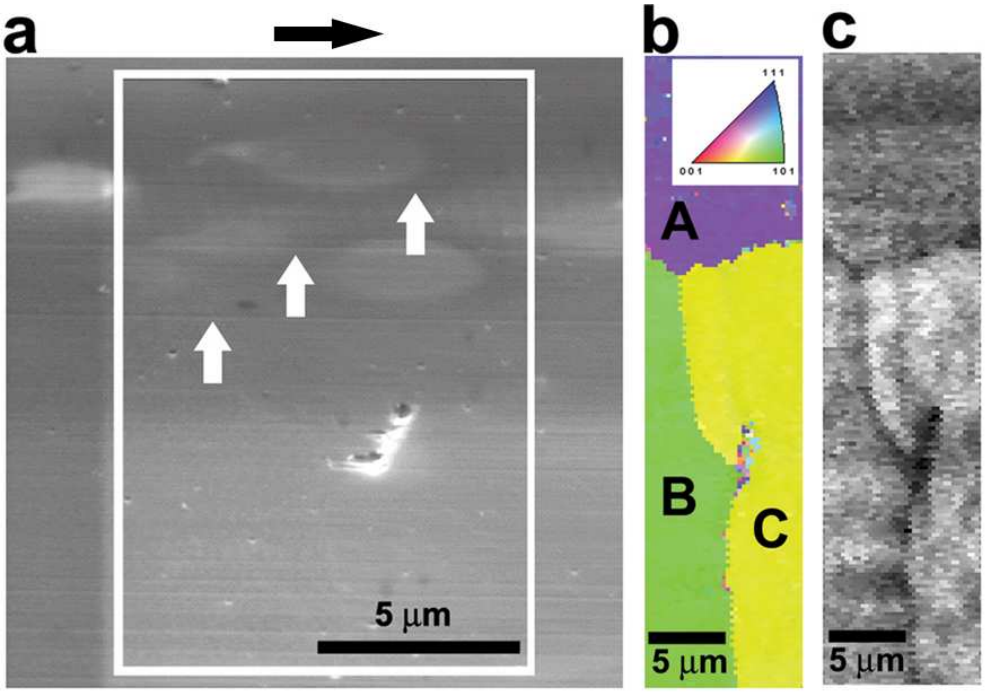

Figure 1 SEM/EBSD investigations for the block-face specimen after ultramicrotomy sectioning at a feed of 30 nm: (a) SEM micrograph tilted 70° indicating the scanned area by EBSD (white rectangle) and marking some knife induced scratches (white arrows); the difference in image contrast is given by electron beam contamination of the sample surface such as the circular features; (b) tilt corrected orientation map [001]; (c) tilt corrected IQ map. The black line indicates the cutting direction.
75x51mm (300 x 300 DPI)

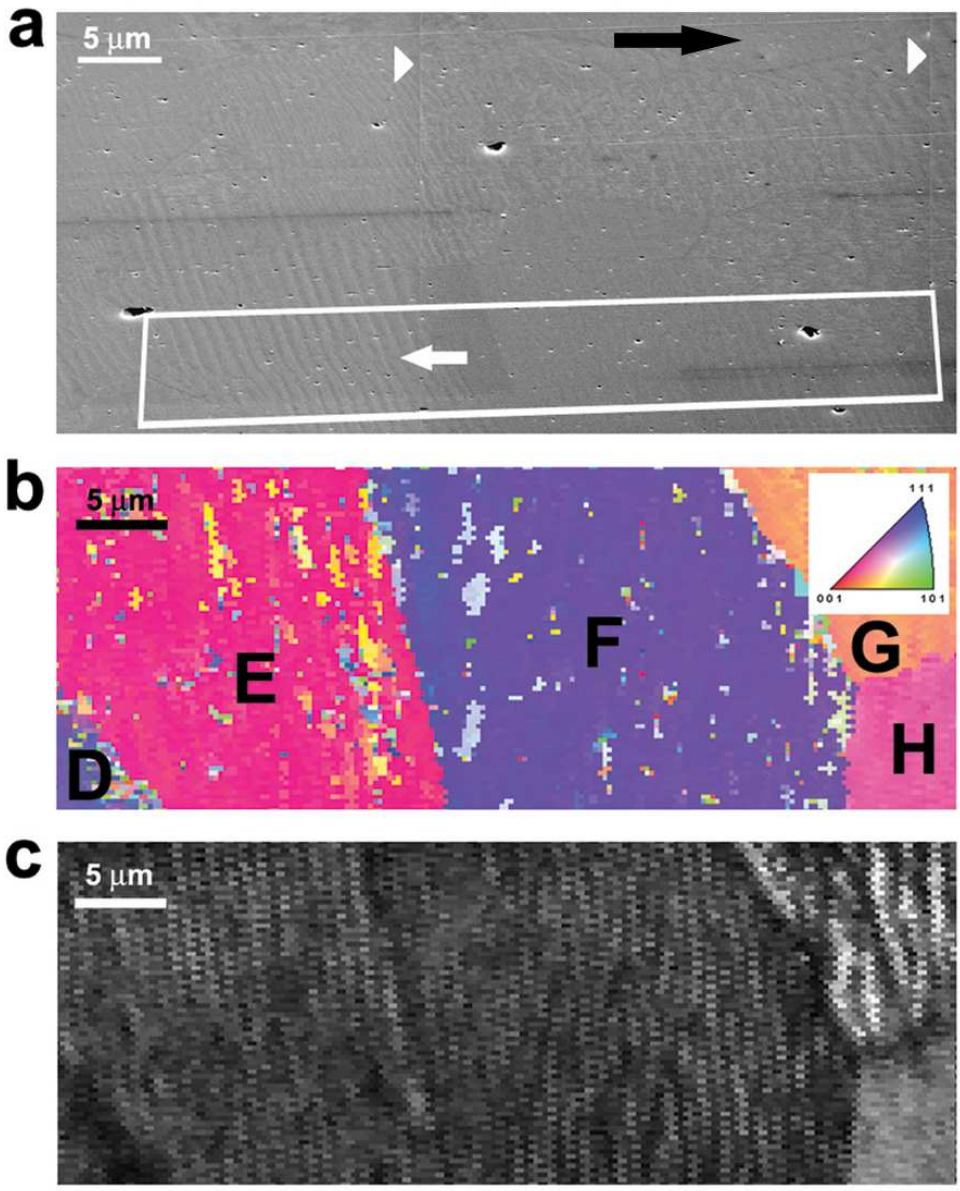

Figure 2 SEM/EBSD investigations for the block-face specimen after ultramicrotomy sectioning at a feed of 1 μm: (a) Series of three consecutive (the white triangles mark the stitching lines) SEM micrographs tilted 70º indicating the scanned area by EBSD (white rectangle); some regions with different contrasts are given by electron beam contamination of the sample surface; (b) tilt corrected orientation map [001]; (c) tilt corrected IQ map. The black line indicates the cutting direction.
75x93mm (300 x 300 DPI)

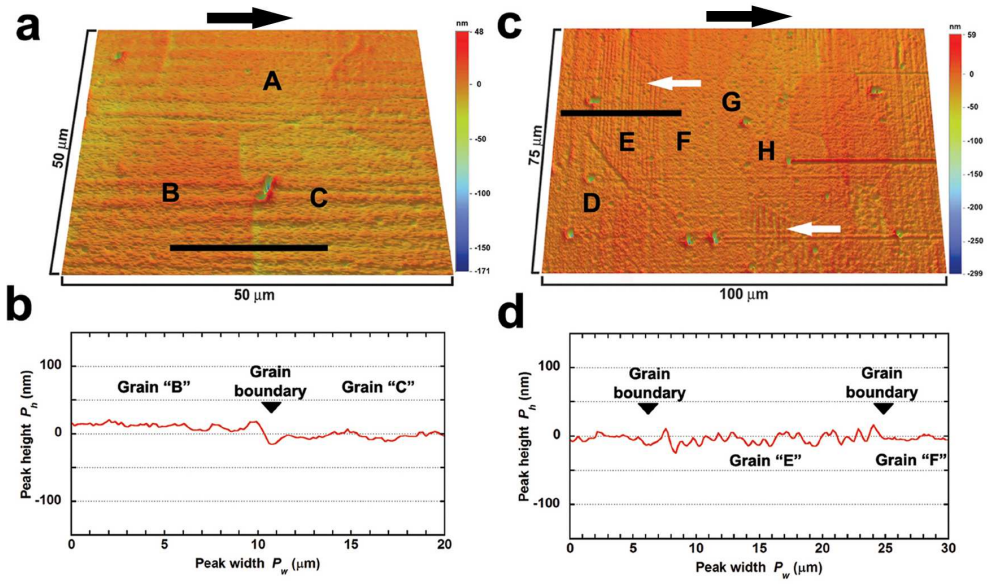

Figure 3 Light interference micrograph and the line profile analysis for the block-face specimens after ultramicrotomy cutting: (a) 3D reconstruction of the sample surface after ultramicrotomy sectioning at a feed of 30 nm; (b) line profile of an area crossing a grain boundary (black bar in (a)); (c) 3D reconstruction of the sample surface after specimen after ultramicrotomy sectioning at a feed of 1 µm; (d) line profile of an area containing a wave-like feature (black bar in (c)). The black lines indicate the cutting direction.
150x87mm (300 x 300 DPI)

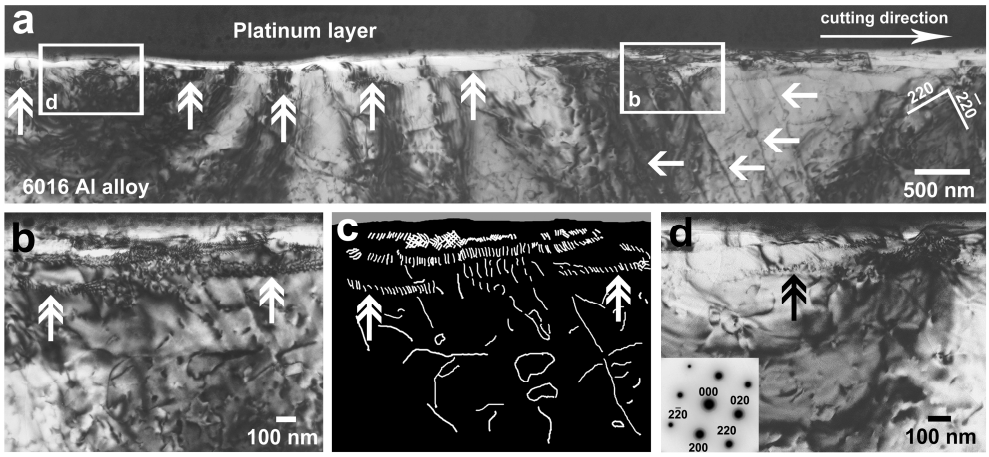

Figure 4 TEM investigations for the block-face specimen after ultramicrotomy sectioning at a feed of 500 nm: (a) bright field micrograph of the cross-sectioned area; (b) high magnification TEM micrograph of a "wave-like feature"; (c) simplified sketch of dislocations distribution in (b) where light grey is Pt layer, black is 6016 Al alloy and white are the dislocations; (d) high magnification TEM micrograph of a "flat" area and selected area diffraction pattern as inset (e^- // $[001]_{Al}$) of the areas in (a), (b) and (d).
149x69mm (600 x 600 DPI)

Table 1 Orientation factor (**m**) for grains "A", "B" and "C" after 30 nm sectioning; for grains "D", "E", "F", "G" and "H" after 1 μm sectioning

Plane	(111)			(-1-11)			(-111)			(1-11)		
Direction	[01-1]	[-101]	[1-10]	[0-1-1]	[101]	[-110]	[01-1]	[101]	[-1-10]	[0-1-1]	[-101]	[110]
30 nm sectioning												
Grain A <4 1 7>{-2 1 1}	0	0	0	0.32	-0.45	0.12	0.49	-0.89	0.40	0.32	-0.12	-0.20
Grain B <-1 -2 13>{-9 11 1}	-0.10	0.09	0.0064	-0.02	0.02	-0.0021	0.68	-0.54	-0.13	-0.44	0.57	-0.12
Grain C <-10 1 5>{-1 0 -2}	-0.19	0.72	-0.53	-0.09	-0.07	0.17	-0.06	-0.07	0.14	-0.29	0.72	-0.43
1 μm sectioning												
Grain D <2 14 19>{-2 3 -2}	-0.02	0.07	-0.05	-0.41	0.26	0.15	0.06	-0.26	0.2	-0.96	0.49	0.47
Grain E <-31 4 7>{1 6 1}	0.05	-0.62	0.57	-0.13	-0.29	0.43	0.03	0.29	0.33	-0.09	0.31	-0.22
Grain F <2 14 19>{-2 3 -2}	-0.02	0.07	-0.05	-0.41	0.26	0.15	0.06	-0.26	0.2	-0.96	0.49	0.47
Grain G <4 -2 1>{13 4 -44}	-0.15	-0.15	0.3	0.11	0.58	-0.7	-0.3	0.51	-0.23	0.06	-0.2	0.13
Grain H <27 7 8>{-3 9 2}	0.01	0.21	-0.22	-0.08	0.2	-0.11	0.01	-0.7	0.68	-0.21	-0.27	0.48

Table 1 Orientation factor (**m**) for grains "A", "B" and "C" after 30 nm sectioning and for grains, "D", "E", "F", "G" and "H" after 1 μm sectioning
270x203mm (96 x 96 DPI)